Nuclear Engineering and Technology 53 (2021) 19–29

Contents lists available at ScienceDirect

Nuclear Engineering and Technology

journal homepage: www.elsevier.com/locate/net

Original Article

Validation of UNIST Monte Carlo code MCS for criticality safety calculations with burnup credit through MOX criticality benchmark problems

Duy Long Ta [a], Ser Gi Hong [a, *], Deokjung Lee [b]

[a] Department of Nuclear Engineering, Hanyang University, 222 Wangsimni-ro, Seongdong-gu, Seoul, 04763, Republic of Korea
[b] Department of Nuclear Engineering, Ulsan National Institute of Science and Technology, UNIST-gil 50, Ulsan, 44919, Republic of Korea

ARTICLE INFO

Article history:
Received 17 April 2020
Received in revised form
2 June 2020
Accepted 10 June 2020
Available online 29 June 2020

Keywords:
Spent fuel cask
Critical experiment
MCS
Validation
MCNP6

ABSTRACT

This paper presents the validation of the MCS code for critical safety analysis with burnup credit for the spent fuel casks. The validation process in this work considers five critical benchmark problem sets, which consist of total 80 critical experiments having MOX fuels from the International Criticality Safety Benchmark Evaluation Project (ICSBEP). The similarity analysis with the use of sensitivity and uncertainty tool TSUNAMI in SCALE was used to determine the applicable benchmark experiments corresponding to each spent fuel cask model and then the Upper Safety Limits (USLs) except for the isotopic validation were evaluated following the guidance from NUREG/CR-6698. The validation process in this work was also performed with the MCNP6 for comparison with the results using MCS calculations. The results of this work showed the consistence between MCS and MCNP6 for the MOX fueled criticality benchmarks, thus proving the reliability of the MCS calculations.

1. Introduction

The safe management of the long-lived nuclides from the spent nuclear fuel is one of the most important problems in nuclear industry. In South Korea, all the PWR spent fuels have been stored in spent fuel storage pools, but many of the spent fuel storage pools are expected to be saturated within about eleven years. Therefore, the dry storage of PWR spent fuels is considered as an interim solution before the permanent disposal in a geological repository or reprocessing. Many researches have been conducted on analysis of spent fuel cask [1–14] in the past few decades, where the criticality evaluations [1,4,6], thermal evaluations [2,3,9] and shielding analyses [5,11] have been credited. From the view point of criticality analysis, the dry storage cask must be designed to guarantee the sub-criticality condition with the requirement that the effective neutron multiplication factor (k_{eff}) does not exceed 0.95 [15], including all biases and bias uncertainties. In order to ensure the subcritical margin on k_{eff}, the critical safety analysis (CSA) should be performed for the spent fuel cask. The burnup credit has been used in CSA to expand the spent fuel cask capacity and the allowable loading range of spent fuels by considering the reactivity reduction resulted from the net consumption of fissile nuclides and production of fission products having high thermal neutron absorption cross sections. In particular, the biases and bias uncertainties in CSA with burnup credit were mainly classified into two different types: (1) biases and bias uncertainties related to uncertainties in nuclear data and computational method in estimating k_{eff}, and (2) the ones from the estimation of spent fuel isotopic compositions in depletion code [16]. Typically, both of these biases and bias uncertainties can be quantified by comparatively analyzing the results from critical experiments including radiochemical assays and computer code calculations.

In this work, the validation of the capability in CSA with burnup credit for spent fuel casks was performed using the Monte Carlo transport code MCS [17,18] for the evaluation of the only first type biases and bias uncertainties (i.e., the ones related to nuclear data and computational methods in estimating k_{eff}) with three specific cask models: TN-32, KN-12 and KN-18, which have been used in South Korea. The transport code MCS is a 3D continuous energy neutron and gamma transport code based on the Monte Carlo method, which was developed by the Computational Reactor Physics and Experiment Laboratory of Ulsan National Institute of

* Corresponding author. Department of Nuclear Engineering, Hanyang University, Wangsimni-ro, Seongdong-gu, Seoul, 04763, Republic of Korea.
E-mail address: hongsergi@hanyang.ac.kr (S.G. Hong).

https://doi.org/10.1016/j.net.2020.06.016

Science and Technology (UNIST). The MCS code, as well as other codes based on Monte Carlo method has the advantage for modeling the complicated structures of spent fuel cask and critical experiment configurations with the capability in flexible 3D geometry modeling and the use of continuous energy neutron cross-section.

The validation process in this work was conducted by following the recommendation of two U.S. Nuclear Regulatory Commission reports (i.e., NUREG/CR-6698 and NUREG/CR-7109): the former [19] was generally considered as a reference for the validation of computational tools with the biases and bias uncertainties in CSA and the latter is a good standard reference for quantifying the biases and bias uncertainties of k_{eff} in actinide and fission product burnup criticality safety analyses [16]. Due to the limitation of the experiments with fission product (FP) and minor actinide (MA) nuclides, five critical problem sets with MOX fuels [20] which consist of 80 critical experiment configurations were considered in this work. These critical problems were used to evaluate the biases and bias uncertainties related to the plutonium isotopes and other major actinides while the bias and bias uncertainty for FP and MA nuclides were considered with a simple conservative method [21]. In this work, we did not consider the bias and bias uncertainty related to the isotopic depletion which will be considered as a separate work in the future.

The validation process of the computational method using MCS code in this work was performed to establish the Upper Safety Limit (USL) (without consideration of isotopic bias and bias uncertainty) for three cask models (i.e., TN-32, KN-12 and KN-18) with the following four steps: (1) consideration of a list of MOX fuel benchmark problems from International Handbook of Evaluated Criticality Safety Benchmark Experiment (ICSBEP); (2) similarity analysis to select the applicable experiments for each spent fuel cask model by using sensitivity/uncertainty tools in SCALE code package; (3) determination of the additional margin to explain the cross section uncertainties related to the FP and MA nuclides because the selected benchmark problems do not consider these nuclides; (4) determination of the USL (without consideration of isotopic bias and bias uncertainty) for each cask model using the criticality result of the critical experiments and the additional margins. In addition, the calculations in this work were also performed by using the Monte Carlo code MCNP6 for comparison with the results obtained from the MCS code. The cask models and the computational tools used in this work are described in Section 2, and Section 3 provides the details of the calculations and the results of the validation process. Finally, the summary and conclusions are given in Section 4.

2. Computational method

2.1. Computational tool

In this work, the validation process was performed with the use of the Monte Carlo code MCS developed by UNIST. The MCS code allows two types of calculations: criticality runs for reactivity calculations and fixed-source runs for shielding problems. There have been two previous works performed on verification and validation of the capability of MCS in transport [18] and shielding calculations [22], while this work is to validate the MCS code for the criticality calculation capability with the MOX fueled criticality benchmark problems for burnup credit application. In this paper, the results obtained from MCS calculations were also compared with the results from MCNP6 [23], which is a general purpose, continuous-energy, generalized-geometry Monte Carlo radiation transport code developed by Los Alamos National Laboratory. All the calculations using MCS and MCNP6 were performed with ENDF/B-VII.r1.

In this work, the sensitivity tool TSUNAMI-3D in SCALE [24] was used to generate sensitivity data files both for the spent fuel cask models and the critical benchmark experiments, which were used in the TSUNAMI-IP module to establish the similarity between each pair of benchmark experiment and cask model. The TSUNAMI-3D calculations were performed using the 238 groups ENDF/B-VII.r0 cross section library provided by SCALE6.1. The SCALE (Standardized Computer Analysis for Licensing Evaluation) code package is a comprehensive modeling and simulation suite for nuclear safety analysis and design that was developed by Oak Ridge National Laboratory.

2.2. Calculation model of spent fuel casks

In this work, the TN-32, KN-12, and KN-18 casks were considered for application of the MCS criticality calculation capability. The TN-32 cask accommodates 32 intact PWR fuel assemblies, with or without burnable poison rod assemblies [25]. In this work, we assumed that the TN-32 cask is loaded with 32 PWR fuel assemblies of 17 × 17 lattice structure, which is comprised of fuel rods having 4.5 wt% initial uranium enrichment, 48 MWd/kg burnup and 5 years cooling time. Each fuel assembly is located inside a fuel basket which is comprised of a 0.2667 cm thick inner stainless steel box surrounded by 0.1016 cm thick borated aluminum absorber plates and a 0.635 cm thick outer aluminum box. The number of absorber plates in each fuel basket depends on the location of the fuel basket inside the cask. The cross sectional view of the TN-32 cask model used in the calculation is shown in Fig. 1, where 32 fuel baskets are placed inside a cavity which has the outer radius of 87.31 cm. The cask body has the inner and outer radii of 87.31 cm and 111.44 cm, respectively. The total height of the TN-32 cask is 467.36 cm, and the thicknesses of the top and bottom regions of the cask are assumed to be 26.67 cm and 26.04 cm, respectively.

The KN-12 transport cask [26,27] was originally designed to transport 12 PWR spent fuel assemblies under wet and dry conditions. In this work, the KN-12 cask model was considered to be loaded with 12 PWR fuel assemblies of 17 × 17 lattice structure, which is comprised of fuel rods having 4.5 wt% initial uranium enrichment at the burnup of 50 MWd/kg and 5 years cooling time. Each fuel assembly is located inside a fuel basket which includes a 0.5 cm thick inner stainless steel box which is covered by a 0.5 cm thick borated aluminum absorber box and a 1.475 cm outer stainless steel box. The cross sectional view of the KN-12 cask is presented in Fig. 2 where 12 fuel baskets are placed inside a stainless steel canister which has the outer radius of 59.6 cm. The cask body has the inner and outer radii of 59.6 cm and 91.1 cm, respectively. We assumed 72 neutron shielding holes inside the cask body where each hole has the diameter of 11 cm and 422 cm in length are filled with air in the calculation model. The total cask height is 480.9 cm including the 30.95 cm thick cask bottom and 31.0 cm thick cask lid.

The KN-18 cask was loaded with 18 PWR fuel assemblies of 16 × 16 type having 4.5 wt% uranium enrichment and 50 GWd/kg burnup with 5 years cooling time. In the spent fuel cask model, each fuel assembly is placed inside a 0.2 cm thick stainless steel fuel basket. The fuel basket is surrounded by four 0.2 cm thick metamic absorber plates of 20 cm wideness and 340 cm height. Fig. 3 presents the cross sectional view of the KN-18 cask model where 18 fuel assembly baskets are placed separately inside the cask. The KN-18 cask is modeled with 516 cm height including 29 cm for the bottom region below the cask and 29 cm upper lid. The inner and outer radii of the cask body are 74.5 cm and 117.95 cm, respectively.

2.3. Critical experiments

In order to validate a computational method applied for the

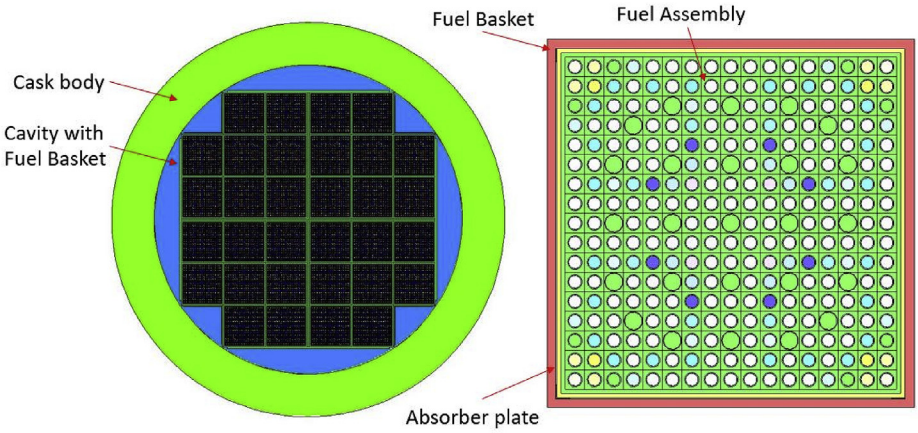

Fig. 1. Cross sectional view of the TN-32 cask model (left) and a fuel assembly basket (right).

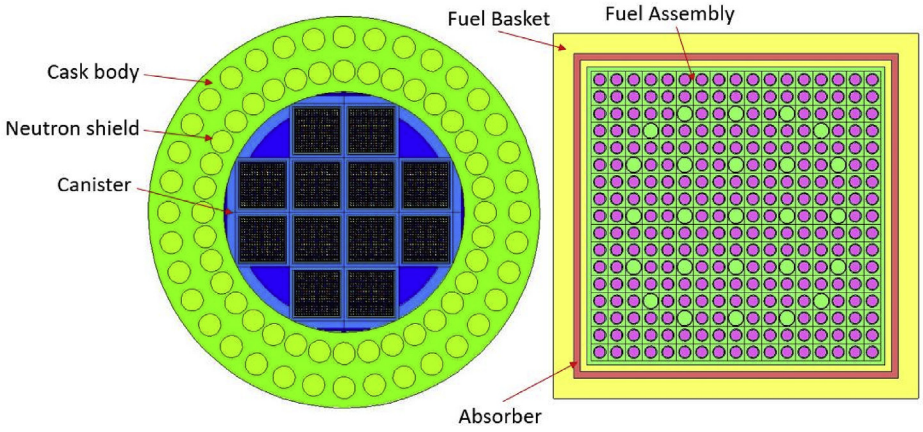

Fig. 2. Cross sectional view of the KN-12 cask model (left) and a fuel assembly basket (right).

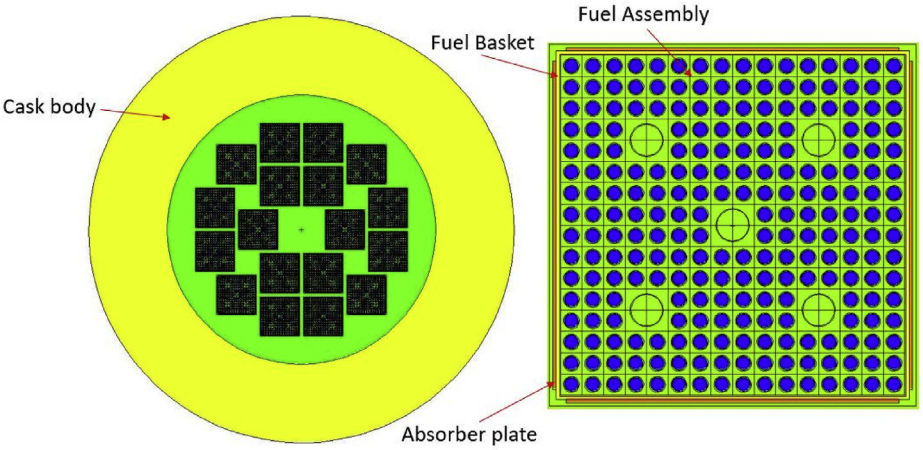

Fig. 3. Cross sectional view of the KN-18 cask model (left) and a fuel assembly basket (right).

spent fuel cask model, the benchmark experiments which have the similar neutronic characteristics to the spent fuel should be considered. In this work, we considered five sets of MOX fuel benchmark experiments having low plutonium contents. These problems are described in International Handbook of Evaluated Criticality Safety Benchmark Experiment (ICSBEP). The analyzed critical benchmark problems in this work have totally 80 problems with identifications ranged from MIX-COM-THERM-002 to MIX-COM-THERM-006. The first three benchmark problem sets comprised of 23 experiments consider square fuel lattices of MOX fuels containing plutonium content ranged from 2.0 wt% to 6.6 wt%. The descritptions on physical parameters are listed in Table 1. The first benchmark problem set is comprised of six critical experiments having 2.0 wt% plutonium content and three different lattice

Table 1
Physical parameters of the square fuel lattice critical experiments.

Problem identification	Experiment number	Pu enrichment (wt%)	Pin pitch (cm)	Number of fuel rod	Fuel lattice	Boron concentration (ppm)	Critical water height (cm)
MIX-COM-THERM-002	1	2.0	1.778	469	–	–	–
	2		1.778	761	–	687.9	–
	3		2.20914	195	–	–	–
	4		2.20914	761	–	1090.4	–
	5		2.51447	161	–	–	–
	6		2.51447	689	–	767.2	–
MIX-COM-THERM-003	1	6.6	1.3208	–	23 × 22	–	82.90
	2		1.4224	–	19 × 19	–	80.80
	3		1.4224	–	21 × 21	337	88.06
	4		1.8679	–	13 × 13	–	68.41
	5		2.0116	–	12 × 12	–	76.76
	6		2.6416	–	11 × 11	–	79.50
MIX-COM-THERM-004	1	3.01	1.825	–	23 × 23	–	59.55
	2		1.825	–	23 × 23	–	61.90
	3		1.825	–	23 × 23	–	64.06
	4		1.956	–	21 × 21	–	61.50
	5		1.956	–	21 × 21	–	64.40
	6		1.956	–	21 × 21	–	69.40
	7		2.225	–	20 × 20	–	60.32
	8		2.225	–	20 × 20	–	62.99
	9		2.225	–	20 × 20	–	65.63
	10		2.474	–	21 × 21	–	62.05
	11		2.474	–	21 × 21	–	64.53

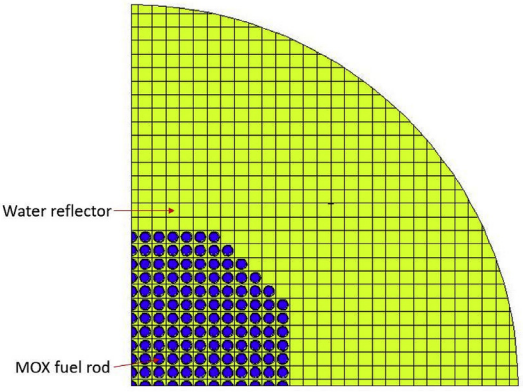

Fig. 4. Representative radial fuel lattice configuration for the first square lattice benchmark problem set (MIX-COM-THERM-002).

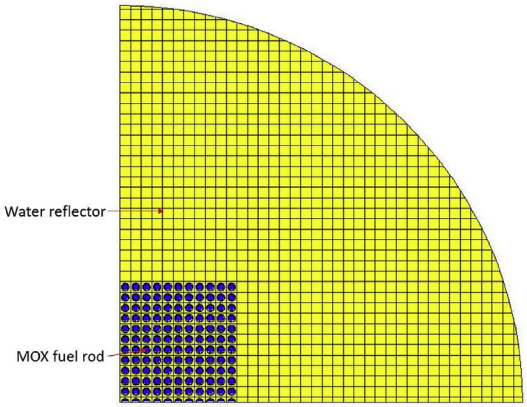

Fig. 5. Representative radial fuel lattice configuration for the second and third square lattice benchmark problem sets (MIX-COM-THERM-003 and -004).

pitches of 1.778, 2.20914 and 2.51447 cm. In this benchmark problem set, the plutonium composition in the fuel rod characterizes a weapon grade plutonium having 0.009 wt% ^{238}Pu, 91.835 wt% ^{239}Pu, 7.76 wt% ^{240}Pu, 0.367 wt% ^{241}Pu and 0.028 wt% ^{242}Pu. Fig. 4 shows a quarter of the radial configuration for the first benchmark problem in this problem set. We considered only a quarter of the configuration due to the symmetry of the benchmark model. As shown in Fig. 4, the fuel rods of square lattice are surrounded by a large amount of water reflector.

The second and third benchmark problem sets are loaded with MOX fuels of 6.6 wt% and 3.01 wt% plutonium contents, respectively. As shown in Fig. 5, the fuel rods are arranged in a square array. The MOX fuel in the second benchmark problem set (i.e., MIX-COM-THERM-003) does not contain ^{238}Pu and it also characterizes a weapon grade plutonium of 90.50 wt% ^{239}Pu, 8.57 wt% ^{240}Pu, 0.89 wt% ^{241}Pu and 0.04 wt% ^{242}Pu. On the other hand, the third benchmark problem set is loaded with a different MOX fuel of 0.49 wt% ^{238}Pu, 68.18 wt% ^{239}Pu, 22.02 wt% ^{240}Pu, 7.26 wt% ^{241}Pu and 2.04 wt% ^{242}Pu. The physical parameters corresponding to each experiment in these two benchmark problem sets are also presented in Table 1. The radial configuration for one representative case is given in Fig. 5, which corresponds to the first experiment of the second benchmark problem set. Table 1 also gives the boron concentrations in water and the water levels for criticality.

The last two benchmark problem sets have hexagonal lattice structures. The first benchmark problem set (i.e., MIX-COM-THERM-005) is loaded with MOX fuel rods of 4.0 wt% plutonium content and their plutonium compositions are 0.28 wt% ^{238}Pu, 75.38 wt% ^{239}Pu, 18.10 wt% ^{240}Pu, 5.08 wt% ^{241}Pu and 1.15 wt% ^{242}Pu. On the other hand, the second set is loaded with a different MOX fuel of 2.0 wt% plutonium content and their plutonium compositions are 0.009 wt% ^{238}Pu, 91.835 wt% ^{239}Pu, 7.76 wt% ^{240}Pu, 0.367 wt% ^{241}Pu and 0.028 wt% ^{242}Pu. The first hexagonal lattice problem set consists of seven critical benchmark problems having different lattice pitches ranging from 2.159 cm to 4.318 cm. On the other hand, the second hexagonal lattice problem set (i.e., MIX-COM-THERM-006) consists of 50 critical benchmark problems. These problems can be classified into two sets. The first set comprised of the first six problems represent the reference cases and the remaining problems are made by replacing the center fuel rod with an absorber rod and adding peripheral fuel rods, where the number of added fuel rods depends on the absorber rod

material. The details of fuel pin pitches and the number of fuel rods for the problem sets of hexagonal lattice are listed in Table 2. A representative fuel lattice configuration is presented in Fig. 6, which is the first experiment of the first hexagonal fuel lattice problem set (i.e, MIX-COM-THERM-005-001).

3. Criticality benchmak analysis

3.1. Determination of applicable benchmark problems

In this sub-section, the similarity indices between the considered critical experiments and each spent fuel cask model are evaluated to select the applicable benchmark problems for each spent fuel cask model. These similarity indices were evaluated by performing sensitivity and uncertainty calculations using the SCALE code by two steps. In the first step, the sensitivity calculation was computed by using the 3D sensitivity tool TSUNAMI-3D of the SCALE for all the benchmark problems and the spent fuel cask models. The sensitivity calculation in TSUNAMI-3D starts with the Monte Carlo calculations for forward and adjoint fluxes, and then the sensitivity coefficient for each nuclide-reaction pair in each energy group is calculated by using the sensitivity module SAMS in TSUNAMI-3D. The sensitivity data calculated using TSUNAMI-3D includes the explicit and the implicit sensitivity coefficients, as shown in Eq. (1). The second term in Eq. (1) expresses the implicit sensitivity coefficient, which considers the first-order implicit effect of perturbations in the material number densities or nuclear data upon the shield group-wise macroscopic cross-section data.

$$S_{k,\Sigma^i_{x,g}} = \frac{\Sigma^i_{x,g}}{k}\frac{dk}{d\Sigma^i_{x,g}} = \frac{\Sigma^i_{x,g}}{k}\frac{\partial k}{\partial \Sigma^i_{x,g}} + \sum_j\sum_h \frac{\Sigma^j_{y,h}}{k}\frac{\partial k}{\partial \Sigma^j_{y,h}} \times \frac{\Sigma^i_{x,g}}{\Sigma^j_{y,h}}\frac{\partial \Sigma^j_{y,h}}{\partial \Sigma^i_{x,g}} \quad (1)$$

where $\Sigma^i_{x,g}$ represents the macroscopic cross-section for reaction x of isotope i in group g, while k and $S_{k,\Sigma^i_{x,g}}$ represent the effective neutron multiplication factor and the sensitivity coefficient for a reaction x of an isotope i in an energy group g, respectively.

In the second step, the TSUNAMI-IP module uses the sensitivity data from TSUNAMI-3D calculations and the cross-section covariance data of SCALE to evaluate the similarity indices for each pair of critical problem and spent fuel cask model. In this work, the integral index c_k which measures the similarity of the systems in terms of related uncertainty was used to represent the similarity between each benchmark problem and each spent fuel cask model. The integral index c_k is defined as

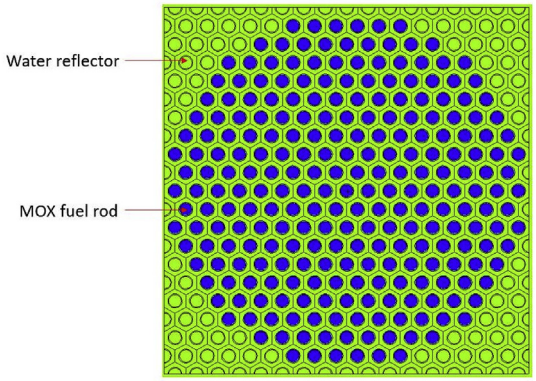

Fig. 6. Representative radial fuel lattice configuration for the hexagonal fuel lattice benchmark problem sets (MIX-COM-THERM-005 and -006).

$$c_k = \frac{\sigma^2_{ij}}{\sigma_i \sigma_j} \quad (2)$$

where σ_i and σ_j are the square roots of the relative variance values of system i and system j, respectively, which correspond to the diagonal elements in the uncertainty matrix calculated by TSUNAMI-IP, and σ^2_{ij} represents the relative covariance between two systems, which corresponds to the off-diagonal elements in the uncertainty matrix. The integral index ck indicates the degree to which two systems share k_{eff} uncertainty due to the nuclear data uncertainties. For examples, a c_k value of zero represents that there is no correlation between two systems, while a c_k value of unity represents a full correlation between systems [16,24]. The similarity results of the critical benchmark problems compared to each spent fuel cask model are presented in Fig. 7. It can be seen that the second benchmark problem set which uses the MOX fuels with highest plutonium content (i.e., 6.6 wt% plutonium content) have the lowest similarity values compared to the other benchmark problem sets due to their hard neutron spectra. Based on the U.S.NRC report [16], the critical experiments with c_k values between 0.8 and 0.9 are considered to be marginally similar, and use of experiments with c_k values below 0.8 is not recommended. Therefore, we only considered the experiments which have c_k values not less than 0.8 as applicable experiments for each spent fuel cask model. From the similarity result in Fig. 7, the numbers of applicable experiments for the TN-32, KN-12 and KN-18 cask model are 69, 78 and 80, respectively.

Table 2
Physical parameters of the hexagonal fuel lattice critical experiments.

Problem identification	Experiment number	Pu enrichment (wt%)	Pin pitch (cm)	Number of fuel rod
MIX-COM-THERM-005	1	4.0	2.159	253
	2		2.362	179
	3		2.667	139
	4		2.903	122
	5		3.520	124
	6		4.064	181
	7		4.318	272
MIX-COM-THERM-006	1	2.0	2.032	320
	2		2.362	192
	3		2.667	152
	4		2.903	148
	5		3.353	163
	6		3.520	180
	7–28		2.667	152–161
	29–50		3.353	163–172

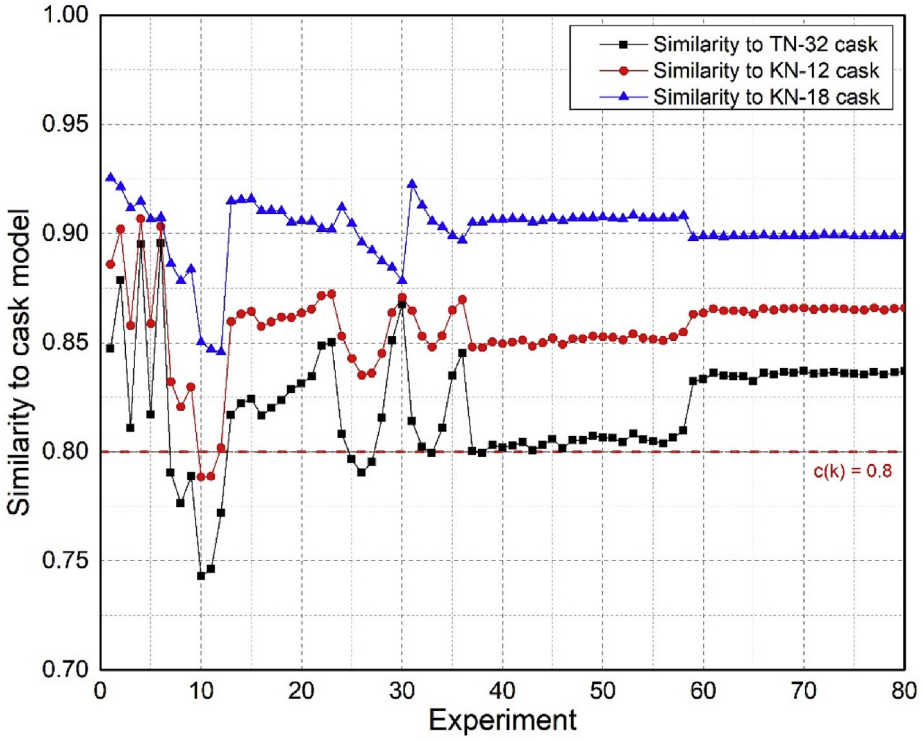

Fig. 7. Similarity analysis result of benchmark experiments to spent fuel cask models.

3.2. Comparative validation of MCS with MCNP6

In this part, the validation procedure and results for three spent fuel casks are presented. At first, criticality calculations are performed with MCS and MCNP6 code for the applicable experiments which have the similarity indices larger than 0.8. Each of the benchmark experiments is calculated with 600 cycles of 20,000 neutron histories each (100 inactive cycles followed by 500 active cycles). The experimental and the calculation results with MCS and MCNP6 for the critical benchmark experiments are presented in Table 3 for the rectangular fuel lattice problems and in Table 4 for hexagonal fuel lattice problems where the maximum statistical standard deviation of MCS and MCNP6 calculations is less than 30 pcm.

The criticality results of MCS and MCNP6 in these two tables show good agreements between the two codes, with small discrepancies of MCS to MCNP6 less than 50 pcm except for few experiments having the differences of 54–104 pcm (cases 25, 27, 54, 59, 62, 72, 73, 75, and 76). The differences of MCS and MCNP6 calculation results to the experimental results are about several hundred pcm except for the last benchmark problem set (i.e., MIX-COM-THERM-006). In the last benchmark problem set, the differences between calculation and experimental results are about few hundred pcm for the first six experiments, while for the remaining ones using a central absorber rod in the fuel lattice, these differences are about 1000 pcm. The maximum discrepancies of MCS and MCNP6 results to the experimental results are 1263 and 1247 pcm, respectively, and the combined RMS uncertainties of the Monte Carlo statistical standard deviation and experiment uncertainties are about 584 pcm. Also, it should be noted that the calculation results give negative bias of ~270 pcm which will be considered in determining USL in the next subsection. These relatively large discrepancies between the calculation and experimental results are due to the fact that the models given in Ref. [20] do not have sufficient information for particulate absorber rods. The calculations were performed with homogeneous absorber rod in this work showed the same trends to the calculation results from Ref. [20], where the k_{eff} values for absorber rod cases are consistently lower than the benchmark model values. The statistics of the discrepancies of MCS and MCNP6 results to the experimental ones over all the considered benchmark problems are summarized in Table 5. The root mean square (RMS) of the discrepancies was calculated using

$$RMS = \sqrt{\frac{1}{n}\sum_{i=1}^{n}\left(k_{cal,i} - k_{exp,i}\right)^2} \tag{3}$$

where $k_{cal,i}$ and $k_{exp,i}$ represent the calculation and experimental results, respectively for the i'th benchmark problem and n is the total number of benchmark problems. The combined RMS uncertainty of the statistical standard deviations in the Monte Carlo calculations and the experimental uncertainties was estimated using

$$std = \sqrt{\frac{1}{n}\sum_{i=1}^{n}\left(\sigma_{exp,i}^2 + \sigma_{cal,i}^2\right)} \tag{4}$$

where $\sigma_{cal,i}$ and $\sigma_{exp,i}$ represent the statistical standard deviation in the Monte Carlo calculations and the experimental uncertainty for the i'th benchmark problem, respectively.

In the following part of this sub-section, the criticality results for those experiments which meet the similarity requirement for each spent fuel cask model were used to determine the USL for these spent fuel casks. Three methods have been introduced for determining the USL in the U.S.NRC report [19]: The single-sided lower tolerance limit, single-side tolerance band, and nonparametric

Table 3
Criticality analysis results for the square lattice benchmark experiments.

Experiment	Benchmark problem	Experimental result	Experiment Uncertainty	MCS result	MCNP result	$\Delta_{MCS-exp}$ (pcm)	$\Delta_{MCNP-exp}$ (pcm)	Discrepancy of MCS to MCNP (pcm)
1	MIX-COM-THERM-002	1.0010	0.0059	1.00060	1.00053	−40.0	−47.0	7.0
2		1.0009	0.0045	1.00181	1.00184	91.0	94.0	−3.0
3		1.0024	0.0029	1.00212	1.00218	−28.0	−22.0	−6.0
4		1.0024	0.0021	1.00633	1.00613	393.0	373.0	20.0
5		1.0038	0.0022	1.00359	1.00357	−21.0	−23.0	2.0
6		1.0029	0.0024	1.00572	1.00585	282.0	295.0	−13.0
7	MIX-COM-THERM-003	1.0000	0.0071	1.00154	1.00141	154.0	141.0	13.0
8		1.0000	0.0057	1.00207	1.00205	207.0	205.0	2.0
9		1.0000	0.0052	1.00156	1.00155	156.0	155.0	1.0
10		1.0000	0.0028	1.00057	1.00051	57.0	51.0	6.0
11		1.0000	0.0024	1.00068	1.00068	68.0	68.0	0.0
12		1.0000	0.002	1.00264	1.00262	264.0	262.0	2.0
13	MIX-COM-THERM-004	1.0000	0.0046	0.99647	0.99620	−352.8	−380.0	27.2
14		1.0000	0.0046	0.99696	0.99704	−304.0	−296.0	−8.0
15		1.0000	0.0046	0.99716	0.99703	−283.7	−297.0	13.3
16		1.0000	0.0039	0.99697	0.99687	−303.0	−313.0	10.0
17		1.0000	0.0039	0.99782	0.99780	−218.4	−220.0	1.6
18		1.0000	0.0039	0.99783	0.99760	−217.4	−240.0	22.6
19		1.0000	0.004	0.99779	0.99771	−220.9	−229.0	8.1
20		1.0000	0.004	0.99829	0.99818	−171.1	−182.0	10.9
21		1.0000	0.004	0.99867	0.99874	−133.1	−126.0	−7.1
22		1.0000	0.0051	0.99831	0.99843	−169.5	−157.0	−12.5
23		1.0000	0.0051	0.99842	0.99841	−157.9	−159.0	1.1

statistical treatment method. The first two methods require a normal statistical distribution of the critical experiment results while the remaining one is used when the critical experiment results are not normally distributed. The experimental result in Table 4 showed that the experimental results are slightly super critical for several benchmark experiments. Therefore, the effective multiplication factor (k_{eff}) for those experiments are normalized [19] by

$$k_{eff,i} = k_{cal,i}/k_{exp,i}. \quad (5)$$

The normalized critical experiment results calculated by Eq. (5) are used to determine if the k_{eff} population for the applicable experiments follows a normal distribution using the Shapiro-Francia normality test [28,29]. The normality test results showed that the k_{eff} populations of the applicable experiments corresponding to all spent fuel cask models do not follow normal distribution. For that reason, the nonparametric statistical treatment (NST) method is used to determine the USL for the spent fuel casks. The USL is determined by

$$USL = K_L - \Delta_{SM} - \Delta_{AOA}, \quad (6)$$

where K_L is the lower limit above which a defined fraction of the true population of k_{eff} is expected to lie [19], Δ_{SM} is the margin of sub-criticality and Δ_{AOA} is the additional margin of sub-criticality resulted from the extension to the area of applicability. By using NST method, the lower limit K_L is computed as follows:

$$K_L = Smallest\ k_{eff}\ value - Uncertainty\ for\ smallest\ k_{eff} - NPM \quad (7)$$

In the above equation, the first component is the smallest normalized k_{eff} among the applicable experiments corresponding to each spent fuel cask. The second one represents the combined uncertainty of Monte Carlo calculation and experimental errors which is calculated with the following equation:

$$\sigma_i = \sqrt{\sigma_{cal,i}^2 + \sigma_{exp,i}^2}. \quad (8)$$

In Eq. (8), NPM is the nonparametric margin which depends on number of considered experiments and it is given in Ref. [19]. In this work, the smallest number of applicable experiments for the spent fuel cask is 69, and so the value of NPM in Eq. (7) is zero. The lower limit K_L values obtained with MCS were estimated to be 0.98290 for three spent fuel cask models. In this work, a value of 0.05 was used as the sub-criticality margin Δ_{SM} [16], and the additional margin Δ_{AOA} was determined to reflect the bias and bias uncertainty in determining k_{eff} related to the FP and MA nuclides. The bias and bias uncertainty in determining spent fuel isotopic compositions in depletion calculation was not considered in this paper, which is planned in a future work. The second term of Δ_{AOA} can be conservatively quantified by a value of 3% of the total worth from the FP and MA nuclides as recommended in Ref. [21], where the total FP and MA nuclides worth is calculated by

$$Total\_worth = k_{eff}^{AFP} - k_{eff}^{AO} \quad (9)$$

The first term of the above equation represents the case where MA and FP nuclides are considered, while the second term represents the case without these nuclides. The total reactivity worth from FP and MA nuclides is calculated with two different k_{eff} calculations with and without considering FP and MA for each cask model. In this work, we analyzed the dependence of that total worth on the burnup by considering the reactivity worth at four different burnups of 20, 30, 40, and 50 MWD/kg. Fig. 8 compares the total reactivity worth of FP and MA at the different burnups for three casks and a comparison between MCS and MCNP6 is also given only for the KN-12 cask. Fig. 8 shows MCS and MCNP6 gives almost the same reactivity worth of FP and MA and the total reactivity worth of FP and MA increases as the burnup. We also analyzed the total worth of FP and MA with different uranium enrichments from 2.0 wt% to 5.0 wt% at the burnup of 50 MWD/kg, which is shown in Fig. 9. Fig. 9 shows that the total reactivity worth of FP and MA increases as the uranium initial enrichment. From the results given in Figs. 8 and 9, 3% of the total worth of FP and MA nuclides with 50 MWD/kg burnup and 5.0 wt% uranium enrichment were estimated to be 365, 310, and 260 pcm for TN-32, KN-12, and KN-18 casks, respectively and they were used to quantify in determining Δ_{AOA} .

Table 4
Criticality analysis results for the hexagonal lattice benchmark experiments.

Experiment	Benchmark problem	Experimental result	Experiment Uncertainty	MCS result	MCNP result	$\Delta_{MCS-exp}$ (pcm)	$\Delta_{MCNP-exp}$ (pcm)	Discrepancy of MCS to MCNP (pcm)
24	MIX-COM-THERM-005	1.0008	0.0022	1.00298	1.00293	218.0	213.0	5.0
25		1.0011	0.0026	1.00104	1.00048	−6.0	−62.0	56.0
26		1.0016	0.0029	1.00746	1.00737	586.0	577.0	9.0
27		1.0021	0.0028	1.00418	1.00358	208.0	148.0	60.0
28		1.0026	0.0036	1.00645	1.0065	385.0	390.0	−5.0
29		1.0033	0.0042	1.00620	1.0063	290.0	300.0	−10.0
30		1.0035	0.0042	1.00765	1.00797	415.0	447.0	−32.0
31	MIX-COM-THERM-006	1.0016	0.0051	0.99880	0.99872	−280.2	−288.0	7.8
32		1.0017	0.0036	1.00210	1.00224	40.0	54.0	−14.0
33		1.0026	0.0036	0.99833	0.99790	−426.9	−470.0	43.1
34		1.0051	0.0044	1.00408	1.00407	−102.0	−103.0	1.0
35		1.0040	0.0054	1.00430	1.00419	30.0	19.0	11.0
36		1.0055	0.0051	1.00209	1.00211	−341.0	−339.0	−2.0
37		1.0024	0.0045	0.99544	0.99530	−696.2	−710.0	13.8
38		1.0035	0.0044	0.99528	0.99524	−821.6	−826.0	4.4
39		1.0035	0.0044	0.99395	0.99410	−954.8	−940.0	−14.8
40		1.0021	0.0044	0.99247	0.99248	−963.3	−962.0	−1.3
41		1.0032	0.0044	0.99242	0.99255	−1078.2	−1065.0	−13.2
42		1.0032	0.0044	0.99187	0.99215	−1132.8	−1105.0	−27.8
43	MIX-COM-THERM-006	1.0021	0.0044	0.99444	0.99430	−765.9	−780.0	14.1
44		1.0026	0.0044	0.99314	0.99338	−945.6	−922.0	−23.6
45		1.0033	0.0044	0.99295	0.99297	−1035.3	−1033.0	−2.3
46		1.0035	0.0045	0.99237	0.99239	−1113.4	−1111.0	−2.4
47		1.0026	0.0046	0.99139	0.99160	−1121.3	−1100.0	−21.3
48		1.0023	0.0045	0.99042	0.99042	−1188.5	−1188.0	−0.5
49		1.0032	0.0045	0.99179	0.99167	−1140.7	−1153.0	12.3
50		1.0033	0.0045	0.99093	0.99103	−1236.7	−1227.0	−9.7
51		1.0030	0.0045	0.99064	0.99053	−1236.0	−1247.0	11.0
52		1.0024	0.0045	0.99035	0.99037	−1204.8	−1203.0	−1.8
53		1.0030	0.0045	0.99092	0.99098	−1207.7	−1202.0	−5.7
54		1.0030	0.0045	0.99037	0.99141	−1263.1	−1159.0	−104.1
55		1.0024	0.0045	0.99091	0.99095	−1148.6	−1145.0	−3.6
56		1.0021	0.0045	0.99037	0.99021	−1173.1	−1189.0	15.9
57		1.0033	0.0045	0.99116	0.99160	−1213.9	−1170.0	−43.9
58		1.0033	0.0046	0.99191	0.99142	−1138.8	−1188.0	49.2
59		1.0040	0.0087	0.99827	0.99898	−573.4	−502.0	−71.4
60		1.0043	0.0087	0.99768	0.99810	−661.7	−620.0	−41.7
61		1.0045	0.0087	0.99746	0.99736	−703.8	−714.0	10.2
62	MIX-COM-THERM-006	1.0037	0.0087	0.99557	0.99633	−813.2	−737.0	−76.2
63		1.0043	0.0087	0.99523	0.99568	−907.0	−862.0	−45.0
64		1.0037	0.0087	0.99451	0.99462	−918.9	−908.0	−10.9
65		1.0044	0.0087	0.99768	0.99750	−672.0	−690.0	18.0
66		1.0036	0.0087	0.99615	0.99621	−745.5	−739.0	−6.5
67		1.0041	0.0087	0.99547	0.99583	−863.3	−827.0	−36.3
68		1.0044	0.0087	0.99433	0.99480	−1007.1	−960.0	−47.1
69		1.0042	0.0088	0.99297	0.99340	−1123.2	−1080.0	−43.2
70		1.0038	0.0087	0.99244	0.99243	−1135.6	−1137.0	1.4
71		1.0038	0.0087	0.99236	0.99267	−1143.7	−1113.0	−30.7
72		1.0036	0.0087	0.99193	0.99254	−1167.0	−1106.0	−61.0
73		1.0044	0.0087	0.99281	0.99355	−1158.6	−1085.0	−73.6
74		1.0044	0.0087	0.99287	0.99316	−1153.4	−1124.0	−29.4
75		1.0040	0.0087	0.99319	0.99369	−1081.5	−1031.0	−50.5
76		1.0040	0.0087	0.99274	0.99369	−1125.7	−1031.0	−94.7
77		1.0040	0.0087	0.99260	0.99300	−1139.6	−1100.0	−39.6
78		1.0038	0.0087	0.99290	0.99291	−1089.8	−1089.0	−0.8
79		1.0039	0.0087	0.99300	0.99303	−1090.3	−1087.0	−3.3
80		1.0044	0.0087	0.99352	0.99365	−1088.1	−1075.0	−13.1

Table 5
Summary of discrepancies of MCS and MCNP6 to the experimental results.

Parameter	Values	
	MCS	MCNP6
Maximum discrepancy (pcm)	1263.1	1247.0
RMS discrepancy (pcm)	791.0	777.2
Combined RMS uncertainty	584.0	583.9
Bias (pcm)	−268	−270

As discussed in Ref. [16], there is an alternative approach that can be used to estimate the bias and bias uncertainty related to FP and MA nuclides when the critical experiment data is insufficient. This approach first generates the sensitivity data with TSUNAMI-3D and these data are used to produce uncertainty (in Δk_{eff}) related to cross-section data with the covariance data using TSUNAMI-IP module in SCALE. Then, these k_{eff} uncertainties related to FP and MA nuclides cross-section data are used as the bounding bias and bias uncertainty related to those nuclides. The uncertainty calculations for the TN-32, KN-12 and KN-18 cask were performed with the fuel assemblies at 50 MWD/kg burnup and 5.0 wt% initial

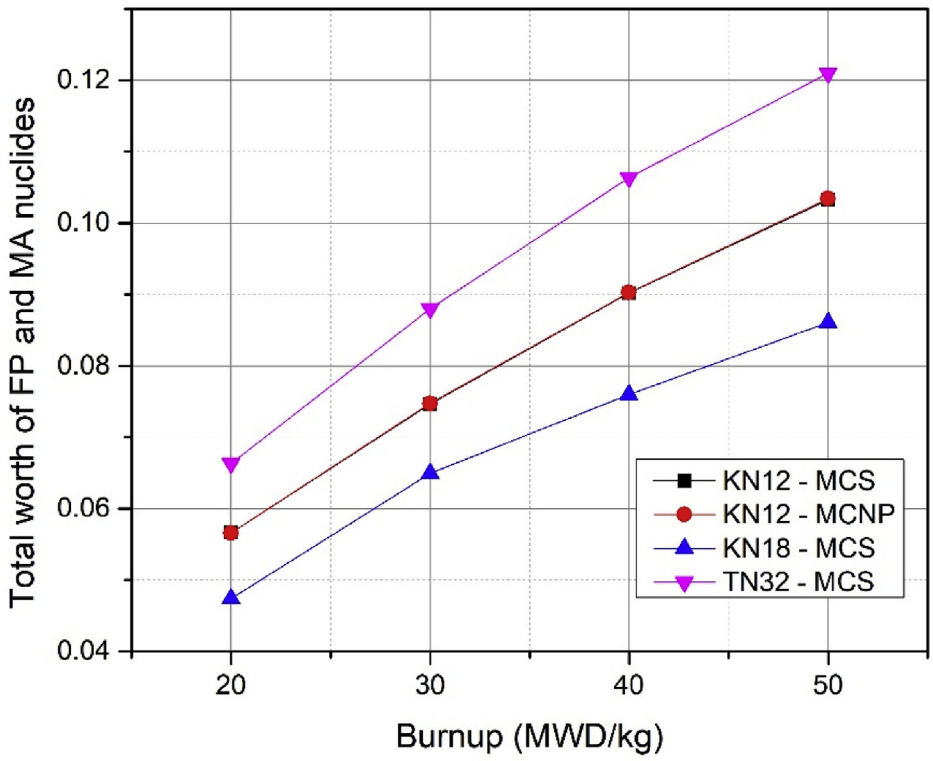

Fig. 8. Total worth of FPs and MAs at several different burn-ups.

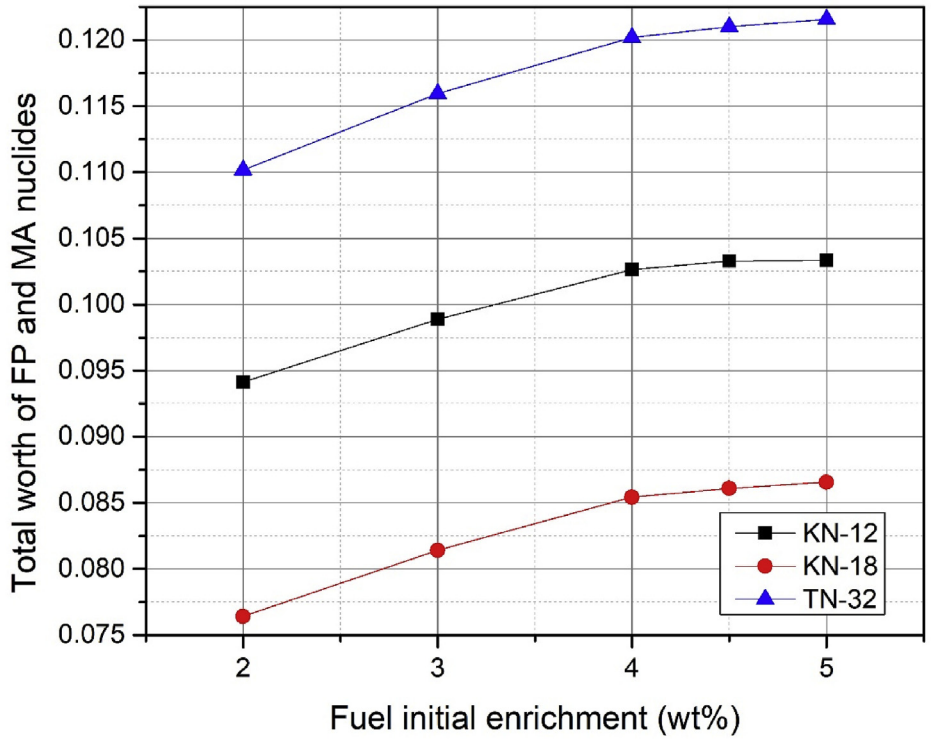

Fig. 9. Total worth of FPs and MAs with different fuel initial enrichment at 50 MWD/kg burn-up.

enrichment to compare with the results determined by using 3% total worth of FP and MA nuclides. The result showed that Δ_{AOA} (i.e., bounding bias and bias uncertainty related to FP and MA) determined by using this approach were estimated to be 330, 284 and 245 pcm for the TN-32, KN-12 and KN18 cask, respectively. These values are slightly lower than the values obtained using 3%

Table 6
Comparison of the USL analysis results for three casks.

	TN-32 cask		KN-12 cask		KN-18 cask	
	MCS	MCNP6	MCS	MCNP6	MCS	MCNP6
Number of considered experiments	69		78		80	
K_L	0.98290	0.98306	0.98290	0.98306	0.98290	0.98306
Δ_{SM}	0.05	0.05	0.05	0.05	0.05	0.05
FP and MA worth	−0.12157	−0.12133	−0.10333	−0.10346	−0.08656	−0.08679
$\Delta_{AOA}(pcm)$	365	364	310	310	260	260
USL	0.92925	0.92942	0.92980	0.92996	0.93030	0.93046

total worth of FP and MA nuclides. Conservatively, we used the bounding biases and bias uncertainties calculated by using the total worth of FP and MA nuclides for the Δ_{AOA} in this work. By using Eq. (6), the USL values are estimated to be 0.92925, 0.92980, and 0.93030 for TN-32, KN-12, and KN-18 casks, respectively. The analysis results with MCS for three spent fuel cask models are summarized in Table 6. The USLs were also determined by the same procedure with the MCNP6 criticality results and the results showed the good agreement with the MCS results. However, it should be noted that these USLs would be considerably reduced with the consideration of the isotopic uncertainties in depletion calculations [13,30].

4. Summary and conclusion

In this work, a criticality analysis was performed to validate the capability of the Monte Carlo code MCS in CSA for burnup credit applications. This work considered five benchmark problem sets comprised of 80 critical experiments having MOX fueled square and hexagonal lattice structures from the ICSBEP critical benchmark book. Also, we estimated the USL values without consideration of the uncertainties related to the isotopic composition using the results of the criticality calculations for three casks (i.e., TN-32, KN-12, and KN-18). In particular, the similarity analyses between each pair of critical experiment and cask have been performed to determine the applicable critical problems using the sensitivity and uncertainty tool TSUNAMI in the SCALE code. The results of the similarity analyses showed that most of the critical experiments both of square and hexagonal lattices except only for few benchmark problems loaded with high plutonium content MOX fuels have the good similarity compared to the cask model.

From the analysis results of the criticality calculations for the critical experiments, it was shown that the discrepancies between MCS and experimental results were mostly about few hundred pcm except for several problems with a different central absorber rod and hexagonal lattice giving a maximum discrepancy of ~1200 pcm. However, these large discrepancies are due to the fact that the information on the modeling data in the reference is not sufficient to model the particulate absorber rod. In addition, the criticality analysis was performed using MCNP6 and the same cross-section library (i.e., ENDF/B-VII.r1). The comparison of the MCS and MCNP6 results showed good agreements with very small discrepancies of less than 50 pcm except for a few benchmark problems having a maximum discrepancy of 104 pcm.

In the last part of this work, the criticality results from MCS and MCNP6 for the applicable critical experiments of each spent fuel cask model were used to determine the USL for the spent fuel cask using the nonparametric statistical treatment method. The USL values using MCS were estimated to be 0.92925, 0.92980, and 0.93030 for TN-32, KN-12, and KN-18 casks, respectively with a typical subcritical margin of 0.05 and an additional margin considering the uncertainty related with FP and MA nuclide cross sections. The additional margin considering the bias related with FP and MA nuclide cross sections were taken as 3% of the total reactivity worth of FP and MA with considerations of various burnup and uranium enrichments. However, the future consideration of the isotopic uncertainties would considerably reduce these USLs.

Declaration of competing interest

The authors declare that they have no known competing financial interests or personal relationships that could have appeared to influence the work reported in this paper.

Acknowledgements

We are very grateful for funding and technical supports from Mr. Ho Cheol Shin and Hwan Soo Lee in Korea Hydro & Nuclear Power Central Research Institute (KHNP-CRI).

Appendix A. Supplementary data

Supplementary data to this article can be found online at https://doi.org/10.1016/j.net.2020.06.016.

References

[1] H.J. Yun, D.Y. Kim, K.H. Park, S.G. Hong, A criticality analysis of the GBC-32 dry storage cask with hanbit nuclear power plant unit 3 fuel assemblies from the viewpoint of burnup credit, Nuclear Engineering and Technology 48 (2016) 624–634.
[2] R. Poskas, V. Simonis, H. Jouhara, P. Poskas, Modeling of decay heat removal from CONSTOR RMBK-1500 casks during long-term storage of spent nuclear fuel, Energy 170 (2019) 978–985.
[3] H.S. Yoo, S.H. Yoo, E.S. Kim, Heat transfer enhancement in dry cask storage for nuclear spent fuel using additive high density inert gas, Ann. Nucl. Energy 132 (2019) 108–118.
[4] D. Price, M.I. Radaideh, D. O'Grady, T. Kozlowski, Advanced BWR criticality safety part II: cask criticality, burnup credit, sensitivity, and uncertainty analyses, Prog. Nucl. Energy 115 (2019) 126–139.
[5] A. Mohammadi, M. Hassanzadeh, M. Gharib, Shielding calculation and criticality safety analysis of spent fuel transportation cask in research reactors, Appl. Radiat. Isot. 108 (2016) 129–132.
[6] M.I. Radaideh, D. Price, T. Kozlowski, Criticality and uncertainty assessment of assembly misloading in BWR transportation cask, Ann. Nucl. Energy 113 (2018) 1–14.
[7] H. Spilker, M. Peehs, H.P. Dyck, G. Kaspar, K. Nissen, Spent LWR fuel dry storage in large transport and storage casks after extended burnup, J. Nucl. Mater. 250 (1997) 63–74.
[8] K.C. Chen, K. Ting, Y.C. Li, Y.Y. Chen, W.K. Cheng, W.C. Chen, C.T. Liu, A study of the probabilistic risk assessment to the dry storage system of spent nuclear fuel, Int. J. Pres. Ves. Pip. 87 (2010) 17–25.
[9] G. Pugliese, R.L. Frano, G. Forasassi, Spent fuel transport cask thermal evaluation under normal and accident conditions, Nucl. Eng. Des. 240 (2010) 1699–1706.
[10] C. Greulich, C. Hughes, Y. Gao, A. Enqvist, J. Baciak, High energy neutron transmission analysis of dry cask storage, Nucl. Instrum. Methods Phys. Res. A 874 (2017) 5.
[11] Y. Gao, N.J. McFerran, A. Enqvist, J.E. Tulenko, J.E. Baciak, Dry cask radiation shielding validation and estimation of cask surface dose rate with MAVRIC during long-term storage, Ann. Nucl. Energy 140 (2020) 107145.
[12] S.E. Smith, X. Sun, C.A. Ford, A.W. Fentiman, MCNP simulation of neutron energy spectra for a TN-32 dry shielded container, Ann. Nucl. Energy 35 (2008) 1296–1300.
[13] H. Yun, K. Park, W. Choi, S.G. Hong, An effective evaluation of depletion

uncertainty for a GBC-32 dry storage cask with PLUS7 fuel assemblies using the Monte Carlo uncertainty sampling method, Ann. Nucl. Energy 110 (2017) 679–691.
[14] A. Rimpler, M. Borst, D. Seifarth, Neutron measurement around a TN-85 type storage cask with high-active waste, Radiat. Meas. 45 (2010) 1290–1292.
[15] Standard Review Plan for Spent Fuel Dry Storage Systems at a General License Facility, NUREG-1536, Revision 1, U.S. Nuclear Regulatory Commission, 2010.
[16] J.M. Scaglione, D.E. Mueller, J.C. Wagner, W.J. Marshall, An Approach for Validating Actinide and Fission Product Burnup Credit Criticality Safety Analyses-Criticality (Keff) Predictions, NUREG/CR-7109, ORNL/TM-2011/514, U.S. Nuclear Regulatory Commission, Oak Ridge National Laboratory, Oak Ridge (TN), 2012.
[17] H. Lee, W. Kim, P. Zhang, M. Lemaire, A. Khassenov, J. Yu, Y. Jo, J. Park, D. Lee, MCS – a Monte Carlo particle transport code for large-scale power reactor analysis, Ann. Nucl. Energy 139 (2020) 107276.
[18] J. Jang, W. Kim, S. Jeong, E. Jeong, J. Park, M. Lemaire, H. Lee, Y. Jo, P. Zhang, D. Lee, Validation of UNIST Monte Carlo code MCS for criticality safety analysis of PWR spent fuel pool and storage cask, Ann. Nucl. Energy 114 (2018) 495–509.
[19] J.C. Dean, R.W. Tayloe Jr., Guide for Validation of Nuclear Criticality Safety Calculational Methodology, NUREG/CR-6698, U.S. Nuclear Regulatory Commission, 2001.
[20] International Handbook of Evaluated Criticality Safety Benchmark Experiments, 2011. NEA/NSC/DOC(95)03.
[21] D.E. Mueller, W.J. Marshall, D.G. Bowen, J.C. Wagner, Bias Estimates Used in Lieu of Validation of Fission Products and Minor Actinides in MCNP K_{eff} Calculations for PWR Burnup Credit Casks, NUREG/CR-7205, U.S. Nuclear Regulatory Commission, Oak Ridge National Laboratory, Oak Ridge (TN), 2015. ORNL/TM-2012/544.
[22] M. Lemaire, H. Lee, B. Ebiwonjumi, C. Kong, W. Kim, Y. Jo, J. Park, D. Lee, Verification of photon transport capability of UNIST Monte Carlo code MCS, Comput. Phys. Commun. 231 (2018) 1–18.
[23] Los Alamos National Laboratory, MCNP6 User's Manual, LA-CP-13-00634, 2013.
[24] Oak Ridge National Laboratory, SCALE: A Comprehensive Modeling and Simulation Suite for Nuclear Safety Analysis and Design, June 2011. ORNL/TN-2005/39, Version 6.1.
[25] Transnuclear, Inc, TN-32 dry storage cask system safety evaluation report. https://www.nrc.gov/docs/ML0036/ML003696918.pdf.
[26] Ju Chan Lee, et al., Usage Inspection of KN-12 Spent Fuel Transport Cask, KAERI/TR-3402/2007, Korea Atomic Energy Research Institute, 2007.
[27] S.H. Chung, et al., Evaluation of the KN-12 spent fuel shipping cask, in: Proceedings of the Korean Nuclear Society Spring Meeting, May 2001. Cheju, Korea.
[28] S.S. Shapiro, R.S. Francia, An approximate analysis of variance test for normality, J. Am. Stat. Assoc. 67 (1972) 215–216.
[29] P. Royston, A pocket-calculator algorithm for the shapiro-francia test for non-normality: an application to medicine, Stat. Med. 12 (1993) 181–194.
[30] G. Radulescu, I.C. Gauld, G. Ilas, J.C. Wagner, An Approach for Validating Actinide and Fission Product Burnup Credit Criticality Safety Analyses – Isotopic Composition Predictions, NUREG/CR-7108, US Nuclear Commission, 2012.